Chemoselective Photodeoxidization of Graphene Oxide Using Sterically Hindered Amines as Catalyst: Synthesis and Applications

Fei Zhao,[†,§,∥] Juqing Liu,[†,‡,§,∥] Xiao Huang,[‡] Xi Zou,[‡] Gang Lu,[‡] Pengju Sun,[†,§] Shixin Wu,[‡] Wei Ai,[†,§] Mingdong Yi,[†,§] Xiaoying Qi,[⊥] Linghai Xie,[†,§,*] Junling Wang,[‡] Hua Zhang,[‡,*] and Wei Huang[†,§,*]

[†]Key Laboratory for Organic Electronics & Information Displays (KLOEID) and Institute of Advanced Materials (IAM), Nanjing University of Posts and Telecommunications, 9 Wenyuan Road, Nanjing 210046, China, [‡]School of Materials Science and Engineering, Nanyang Technological University, 50 Nanyang Avenue, Singapore 639798, Singapore, [§]Jiangsu—Singapore Joint Research Center for Organic/Bio Electronics & Information Displays, 9 Wenyuan Road, Nanjing 210046, China, and [⊥]Singapore Institute of Manufacturing Technology, 71 Nanyang Drive, Singapore 638075, Singapore. [∥]These authors contributed equally to this work.

ABSTRACT

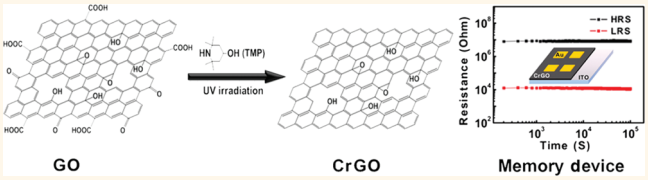

We report a green and efficient method for chemoselective deoxidization of graphene oxide *via* the ultraviolet irradiation catalyzed with 2,2,6,6-tetramethyl-4-piperidinol. While the sp^2-hybridized oxygen functional groups are removed after the reduction, the epoxy and hydroxyl groups are retained in the chemoselectively reduced graphene oxide (CrGO). The obtained CrGO nanosheets exhibit the high solubility and excellent electronic stability, which allows for the fabrication of thin film devices through a solution processing. As a proof of concept, a CrGO-based write-once-read-many-times memory device with the desirable stability and long-time operation is fabricated.

KEYWORDS: graphene oxide · chemoselective reduction · green catalysis · photoreduction · memory devices

As a unique two-dimensional material, graphene has shown many unusual properties and wide applications in electronics, photonics, mechanics, and so on.[1−5] To date, plenty of strategies have been developed to prepare graphene, such as micromechanical exfoliation,[6] CVD growth,[7−9] and plasma etching of multiwalled carbon nanotubes.[10,11] Unfortunately, these methods suffer from the low-throughput, low reproducibility, and/or high cost. Therefore, the use of wet-chemical methods for the exfoliation of graphite[12,13] is more promising due to the low-cost and large-scale production. Recently, the chemical oxidation and exfoliation of graphite[14−17] has been recognized as a leading approach to synthesize graphene oxide (GO), which is a kind of water-soluble,[18,19] chemically active,[20,21] and biocompatible[22−25] graphene derivative. However, the low conductivity of GO restricts its electronic applications.

In order to improve the electrical conductivity, various reduction methods with different reduction agents[26−28] and different reduction conditions[29−33] have been demonstrated to prepare reduced graphene oxide (rGO). However, most of the currently used methods require high temperature, toxic reagents, or vacuum conditions.[34] In addition, although rGO exhibits improved conductivity[35] by restoring partial sp^2-hybridized carbon domains, its solubility in polar solvents is compromised due to the removal of surface functional groups. In order to address this issue, the reduction of GO has been carried out in the presence of polymers or surfactants,[36−38] so that the resulting rGO sheets remain dispersible in many solvents. However, removal of the polymers or surfactants might be required for the further applications. Therefore, to develop a facile reduction method which can retain the solubility of rGO is meaningful to its practical applications.

Recently, we have reported that rGO can be used as electrodes in memory devices.[39,40] Besides this, the graphene-based material, with the tunable band gap through the control of a reduction process of GO,[41] is also an attractive candidate as the active layer in memory devices. Importantly, it was found that the functional groups

* Address correspondence to wei-huang@njupt.edu.cn, iamlhxie@njupt.edu.cn, hzhang@ntu.edu.sg.

Received for review November 23, 2011 and accepted March 15, 2012.

Published online March 15, 2012
10.1021/nn2047185

© 2012 American Chemical Society

on graphene are sensitive to the electrical degradation,[42] which shorten the device lifetime and affect the device stability. Therefore, it is desirable to develop new methods for the fine control of GO reduction in order not only to improve the electronic stability of GO by selective removal of certain functional groups but also to maintain its solubility imparted by the residual oxygen-containing groups.

Herein, we present a photoinduced organo-catalytic method which gives a novel, green, and efficient pathway for reduction of GO. As an example, by using the 2,2,6,6-tetramethyl-4-piperidinol (TMP), which is a member of hindered amine light stabilizers and a nontoxic, water-soluble, and stable catalyst, as the photocatalyst, GO can be selectively photoreduced; that is, the sp^2-hybridized oxygen functional groups on the GO surface can be effectively removed, while the epoxy and hydroxyl groups are retained. Thus, the obtained chemoselectively reduced GO (CrGO) is dispersed in water and some polar solvents, due to the partially remaining oxygen-containing groups on its basal plane.[43] Moreover, we fabricate a nonvolatile write-once-read-many-times (WORM) memory device by using CrGO as the active layer to demonstrate that this chemoselective deoxidization (CD) is an effective strategy to improve the stability of rGO and its electronic devices.

RESULTS AND DISCUSSION

The preparation of chemoselectively reduced graphene oxide (CrGO) is described in the Materials and Methods. As a control experiment, the GO solution was irradiated under the UV light. It was observed that the color of GO solution changed from light brown (inset A of Figure 1) to dark brown (inset B of Figure 1) after 25 min UV irradiation, which was verified by the partial restoration of the π-electrons arising from the deoxidization.[44] However, when 2,2,6,6-tetramethyl-4-piperidinol (TMP) was added into the GO solution, the solution color immediately changed and turned to dark after 25 min UV irradiation, suggesting that the photodeoxidization process was accelerated in the presence of TMP, and CrGO, which will be confirmed in the following paragraphs, was obtained.

Figure 1 shows the UV−vis spectra of GO, UV-irradiated GO, referred to as UV-rGO, and CrGO solutions at the same concentration. It is observed that, with addition of TMP, the intensity of the peak centered at 228 nm, which is characteristic for GO, decreased gradually accompanied with increased absorption in the visible region, indicating that the reduction of GO happened.[45] Meanwhile, the time-dependent deoxidization process of GO in the presence of TMP was further monitored by UV−vis spectroscopy (Figure S1 in Supporting Information (SI)), which confirmed that this photoreduction was very fast.

X-ray photoelectron spectroscopy (XPS) was employed to provide the detailed information on the

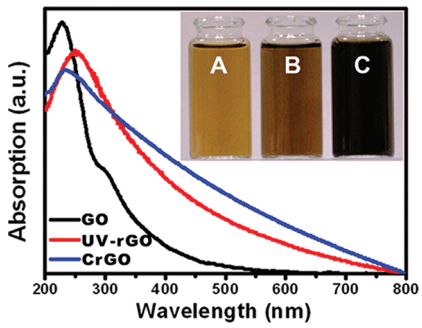

Figure 1. UV−vis spectra and photographs of GO solution (inset A), GO solution after 25 min UV irradiation (*i.e.*, UV-rGO solution, inset B), and 25 min UV-irradiated mixture of GO and TMP followed by removal of TMP (*i.e.*, CrGO solution, inset C).

results of the chemoselective deoxidization (CD). In Figure 2A, the deconvoluted peaks of GO are assigned to epoxy (C−O−C, 285.7 eV), hydroxyl (C−OH, 286.7 eV), carbonyl (C═O, 288.0 eV), and carboxyl (−COOH, 289.1 eV) groups, and the peak centered at the binding energy of 284.6 eV is assigned to the C−C bond.[46] In the experiment of photoreduction of GO without TMP, after 25 min of UV irradiation, all of the oxygen-containing groups were only partially removed because of the decreased peak intensities of epoxy, hydroxyl, carbonyl, and carboxyl groups compared to that of C−C bond (Figure 2B). If TMP was added in the GO solution, after 25 min of UV irradiation, the peak intensities of carbonyl and carboxyl groups were reduced by ~98 and ~100%, respectively (Figure 2C). However, less than 15% reduction of intensities of hydroxyl and epoxy groups was obtained, indicating that the CD process was successfully realized in the TMP-catalyzed photoreduction of GO. Moreover, the value of C1s/O1s atomic ratios of GO, UV-rGO, and CrGO are 2.4, 6.8, and 3.6, respectively, indicating that the CD process presents a desirable selectivity for the reduction of GO.

In order to get the pure CrGO used for the electronic device application, the complete removal of TMP in the final reduced product is necessary. The successful purification of CrGO was confirmed by the Fourier transform infrared (FT-IR) spectroscopy. The typical FT-IR spectrum of GO (curve a in Figure 2D) exhibits stretching vibration peaks of O−H (ν_{O-H} at 3150−3700 cm^{-1}), C═O ($\nu_{C=O}$ at 1730 cm^{-1}), C═C ($\nu_{C=C}$ at 1620 cm^{-1}), and C−O (ν_{C-O} at 1368 cm^{-1} and ν_{C-O-C} at 1110 cm^{-1}),[47,48] while the mixture of CrGO and TMP gives the extra peaks, such as those attributed to N−H (ν_{N-H} at 3420 cm^{-1}) and C−H (ν_{C-H} around 2970 cm^{-1}) from TMP (curve b in Figure 2D). However, in the spectrum of CrGO (curve c in Figure 2D), the strong absorption peaks at 3420 and 2970 cm^{-1} in curve b were eliminated, indicating that the TMP was completely washed away and the CrGO was purified (Figure S2 in SI shows the ^1H NMR and ^{13}C NMR spectra of this extracted TMP, indicating that TMP played the role of

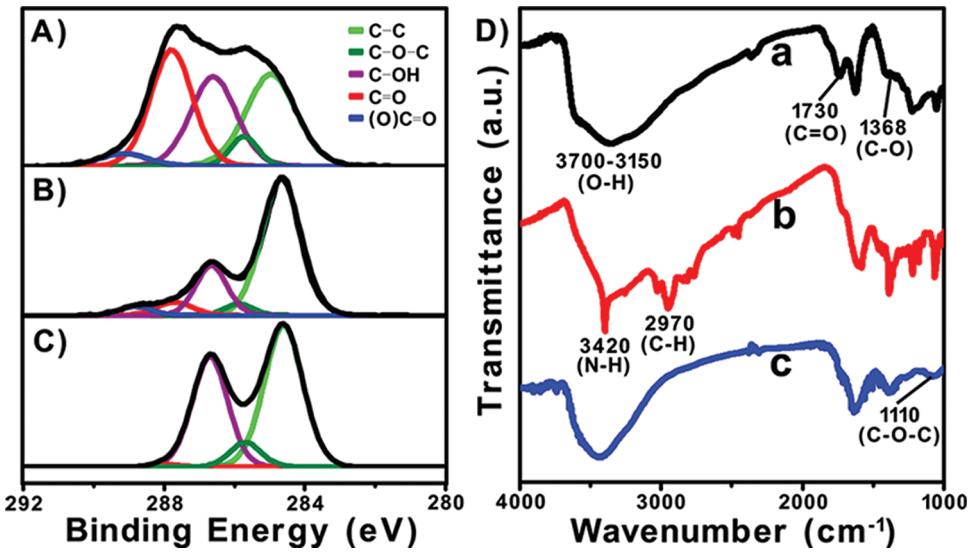

Figure 2. XPS spectra of (A) GO, (B) UV-rGO, and (C) CrGO. (D) FT-IR spectra of GO (a), CrGO before (b) and after (c) removal of TMP.

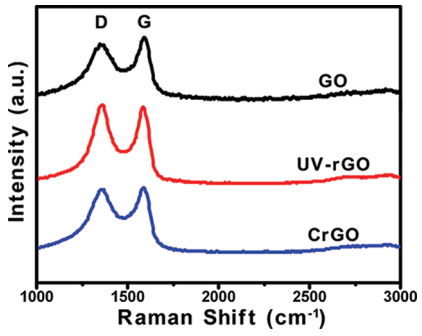

Figure 3. Raman spectra of GO, UV-rGO, and CrGO.

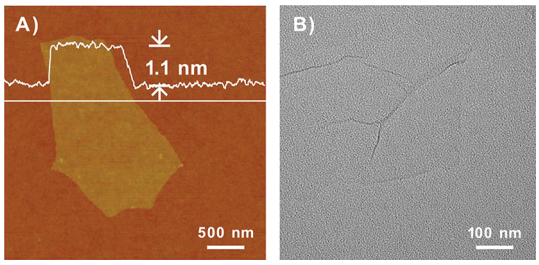

Figure 4. (A) AFM image and (B) TEM image of purified CrGO nanosheets.

catalyst in the CD process). In addition, the peak at 1730 cm^{-1} disappeared, suggesting that the C═O group was completely reduced in CrGO. Moreover, the hydroxyl and epoxy groups in CrGO were effectively protected as shown in the peaks at 1368 and 1110 cm^{-1}, respectively. These results are consistent with those obtained by XPS (Figure 2C).

The Raman spectra of GO, UV-rGO, and CrGO are shown in Figure 3. Obviously, the D band and G band are centered at 1340 and 1580 cm^{-1}, respectively, while the small but perceptible 2D band and S3 band appeared around 2700 and 2930 cm^{-1} (Figure S3A in SI), respectively.[49] Generally, the Raman D/G intensity ratio (I_D/I_G) is proportional to the average size of the sp^2 domains.[50] The UV-rGO has higher I_D/I_G value (1.03) compared to that of GO (0.88) and CrGO (0.93), as shown in Figure 3, meaning the partial restoration of the π-conjugated structures in the GO nanosheets by UV irradiation.[44] However, due to the efficient protection of hydroxyl and epoxy groups, the I_D/I_G value of CrGO (0.93) is only slightly larger than that of GO (0.88). In a control experiment, the hydrazine-reduced GO (HrGO) exhibits the highest I_D/I_G (1.14, in Figure S3B). Moreover, the I_{2D}/I_G was introduced to further evaluate the reduction ability.[51] The I_{2D}/I_G ratios of GO, UV-rGO, and CrGO are 0.101, 0.135, and 0.108, respectively, indicating that the reduction degree of CrGO is lower than that of UV-rGO. It is consistent with the XPS results; that is, more oxygen-containing groups were retained in CrGO. The slight increase of the I_{2D}/I_G value of CrGO (0.108) compared to GO (0.101) should be attributed to the removal of carboxyl and carbonyl groups.[52]

If the residual hydroxyl and epoxy groups decorate the basal plane of graphene sheet, the similar thickness and solubility of CrGO, as compared to GO, are thereby expected. Topographic analysis of CrGO was carried out by atomic force microscopy (AFM). A typical CrGO nanosheet shows a thickness of about 1.1 nm (Figure 4A), which is similar to the thickness of the original GO nanosheet (Figure S4 in SI), suggesting that CrGO is a single-layer sheet decorated with hydroxyl and epoxy groups as confirmed above.[53] Moreover, the obtained CrGO nanosheets exhibited the excellent solubility in water and several polar solvents (Figure S5). Evidently, the single-layer CrGO nanosheets, instead of stacked ones, were observed by TEM after placing a droplet of CrGO solution on a copper grid followed by drying (Figure 4B).

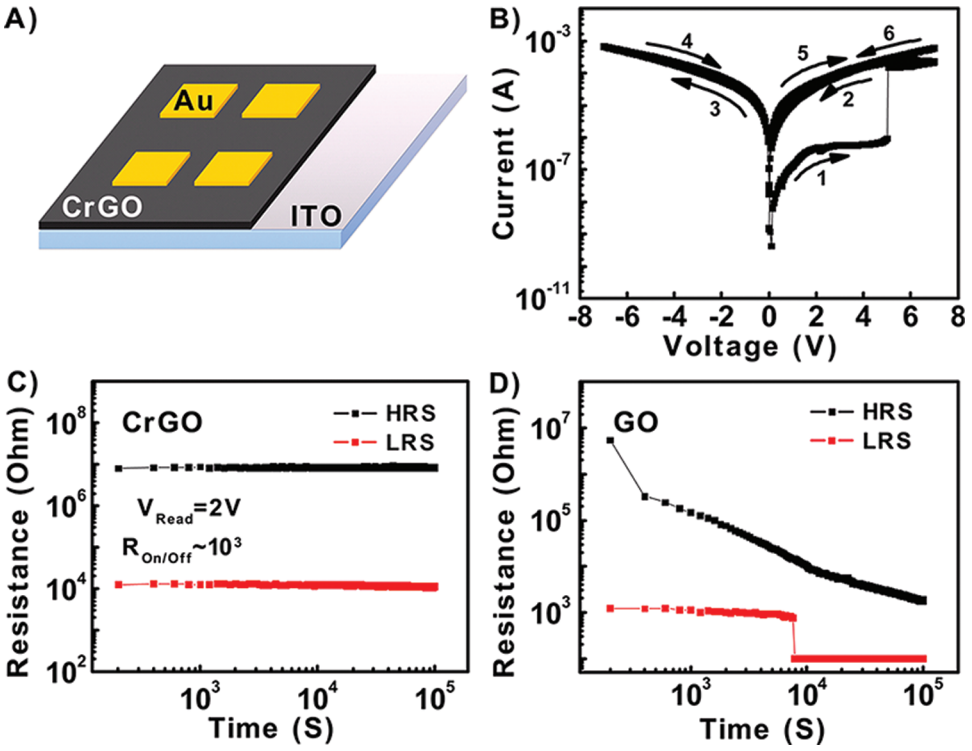

Figure 5. (A) Schematic illustration of the Au/CrGO (30 nm)/ITO memory device. (B) Typical *I*–*V* curve of the memory device in (A). (C) Retention test of the device in (A), read at 2 V without disturbance for around 10^5 s. (D) Retention test of the Au/GO(30 nm)/ITO memory device, in which a permanent breakdown occurred.

Due to the strong electrochemical activity and hydrophilicity of carboxyl group, the decarbonylated GO (*i.e.*, the CrGO here) is considered as a promising stable electroactive material as compared to GO. The thermogravimetric analysis (TGA) shows that CrGO has higher thermal stability than GO (Figure S6). To further confirm the improved stability of CrGO after the CD process, a typical device with the configuration of Au/CrGO (30 nm)/ITO was fabricated (Figure 5A), where the CrGO film acted as the electroactive layer. Its current–voltage property and retention characterization were studied in detail. The CrGO-based device exhibited the electrical bistable behavior, with a memory effect of write-once-read-many-times (WORM) (Figure 5B). The switch voltage, as the transition from high resistance state (HRS, off state) to low resistance state (LRS, on state), is about 5 V. The high on/off current ratio of 10^3 promises a low misreading during operation, which is comparable with that of GO-based memory.[54] The unerase operation under a reverse bias is attributed to an irreversible breakdown of the oxygen-containing functional groups of CrGO, instead of forming metal oxides at the interface between electrodes and CrGO due to the chemical inertness of Au. Most importantly, the CrGO-based memory devices exhibited an excellent stability and no significant degradation in both HRS and LRS, which were investigated by a 10^5 s of continuous retention test at 2 V (Figure 5C).

In a control experiment, the GO-based device with the same configuration was prepared and characterized. Compared to the CrGO-based memory device, the GO-based memory device exhibited poor stability. An obvious degradation in both HRS and LRS was observed under the same retention test (Figure 5D), which limits the practical use of GO as a functional material in the device applications. The reason is that CrGO (*i.e.*, the decarbonylated GO) contains less active and hydrophilic carboxyl and carbonyl groups, compared to GO, implying that the residual oxygen-containing functional groups on CrGO are more stable. Therefore, the CD process offers an effective strategy to improve the stability of GO-based materials in electronic devices. In addition, the obtained CrGO provides a new platform to create stable carbon-based semiconductor devices, particularly in the data storage field, with the advantage of stable operation, permanent lifetime, and low misreading probability.

CONCLUSION

In conclusion, a chemoselective deoxidization (CD) process has been successfully achieved by using an efficient, low-cost, and nontoxic photocatalytic method. The obtained chemoselectively reduced graphene oxide (CrGO) shows the high solubility and outstanding electrical stability, allowing for the solution-processed fabrication of stable electronic devices.

CrGO-based thin film device (Au/CrGO/ITO) exhibits the WORM-type memory effect with a desirable service lifetime. We believe that the CD strategy can be extensively applied in the selective modification of various carbon-based materials and polymers to obtain the stable carbon-based semiconductor composites.

MATERIALS AND METHODS

Materials. Graphite powder (325 mesh) was purchased from Baichuan Graphite Co., Ltd. (Qingdao, China). Sulfuric acid (H_2SO_4), sodium nitrate ($NaNO_3$), potassium permanganate ($KMnO_4$), potassium persulfate ($K_2S_2O_8$), phosphorus pentoxide (P_2O_5), hydrogen peroxide (H_2O_2), hydrochloric acid (HCl), and 2,2,6,6-tetramethyl-4-piperidinol (TMP) were purchased from Sinopharm Chemical Reagent Co., Ltd. (Shanghai, China). Unless otherwise specified, all reagents were used without further purification.

Preparation of Graphene Oxide (GO). GO was prepared by the modified Hummers method.[55,56] Briefly, the graphite powder (0.5 g) was mixed with 3 mL of 98% H_2SO_4, 0.5 g of $K_2S_2O_8$, and 0.5 g of P_2O_5 at 80 °C for 4.5 h. Then the obtained powder was washed by DI water and dried. The product mixed with 20 mL of 98% H_2SO_4 and 0.5 g of $NaNO_3$ followed by slowly adding 2.5 g of $KMnO_4$. Note that, during the addition of $KMnO_4$, an ice bath should be used in order to avoid the overheating and explosion. The solution temperature was increased to 40 °C, which was then maintained for 2 h. Then 10 mL of 30% H_2SO_4, 40 mL of H_2O, and 5 mL of 30% H_2O_2 were added sequentially. Finally, the product was purified by centrifuge washing three times with 1 M HCl and three times with DI water. The purified GO was dried in a vacuum drier to get GO powder.

Preparation of Chemoselective Reduced Graphene Oxide (CrGO). The GO powder (30 mg) was added to 100 mL of TMP aqueous solution (0.3 mg/mL). The mixture was sonicated for 15 min. The obtained solution was transferred into a culture flask and exposed to the ultraviolet irradiation with violent stir for 25 min. Then, the obtained black liquid was dumped into a separating funnel. Twenty milliliters of toluene was used to extract the TMP, and the extraction procedure was repeated 3−5 times. Finally, the obtained CrGO was dried in a vacuum drier.

Fabrication of Memory Devices. CrGO film was fabricated on a precleaned ITO glass substrate by spin-coating of 180 μL of CrGO ethanolic solution (0.8 mg/mL) at 3000 rpm under ambient conditions. The obtained CrGO film was dehydrated under vacuum at 30 °C for 30 min to obtain a *ca.* 30 nm thick film. In a control experiment, the 100 μL GO methanolic solution (0.8 mg/mL) was spin-coated on ITO at 3000 rpm under ambient conditions to obtain a *ca.* 30 nm GO film, which was also dehydrated under vacuum at 30 °C for 30 min. Finally, a 60 nm top Au electrode was deposited onto the CrGO or GO films by thermal evaporation under vacuum to obtain the Au/CrGO (30 nm)/ITO and the Au/GO (30 nm)/ITO devices, respectively.

Characterization. The UV−vis spectra were performed using Shimadzu UV-3600 spectrometer with correction for the solvent background. Fourier transform infrared (FT-IR) spectra were recorded using an IR-Prestige-21 FT-IR spectrophotometer with a mid-IR (MIR) globar source. Samples for infrared measurements were predried in vacuum. Ultraviolet light was performed with a MEJIRO GENOSSEN MUA-165 (365 nm, 230 W, 3800 mW/cm^2). The Raman measurement was carried out on a WITec CRM200 confocal Raman microscopy system (WITec Instruments Corp, Germany) with excitation line of 633 nm and an air cooling charge-coupled device (CCD). The Raman band of a silicon wafer at 520 cm^{-1} was used as a reference to calibrate the spectrometer. The thermogravimetric analysis (TGA) was carried out in a TGA-50 (Shimadzu) at a heating rate of 10 °C min^{-1} under N_2 gas flow (20 mL min^{-1}). Atomic force microscopy (AFM, Dimension 3100 Veeco, CA) was performed in tapping mode with a Si tip (resonance frequency = 320 kHz; spring constant = 42 N m^{-1}) at a scanning rate of 1 Hz. For transmission electron microscopy (TEM, NOVA NANOTEM 600) analysis, CrGO solution was drop-casted onto a copper grid and imaged in high vacuum mode. Core-level X-ray photoelectron spectroscopy (XPS) measurements were carried out (with Al Kα radiation, 1486.6 eV) using a VSW EA45 analyzer at 100 eV pass energy for dried solid samples of GO, CrGO, and the mixture of CrGO and TMP. C1s and O1s peaks were analyzed. The *I*−*V* measurements were performed by Hewlett-Packard 4156B semiconductor parameter analyzer under ambient conditions.

Conflict of Interest: The authors declare no competing financial interest.

Acknowledgment. This work was supported by the "973" project (2009CB930600), NNSFC (Grants 60876010, 60706017, and 20774043), the Key Project of Chinese Ministry of Education (No. 208050), the NSF of Jiangsu Province (Grants 07KJB150082, BK2008053, 08KJB510013, and SJ209003), the Research Fund for Postgraduate Innovation Project of Jiangsu Province (CX08B_083Z) and NJUPT (NY210030); the AcRF Tier 2 (ARC 10/10, No. MOE2010-T2-1-060) from MOE, CREATE program (Nanomaterials for Energy and Water Management) from NRF, and New Initiative Fund FY 2010 (M58120031) from NTU in Singapore. The authors acknowledge Prof. Hui Xu (Key Laboratory of Functional Inorganic Material Chemistry (MoE), Heilongjiang University) for the TEM characterization, Dr. Yanwen Ma (KLOEID and IAM, Nanjing University of Posts and Telecommunications) and Ms. Xuan Yin (School of Materials Science and Engineering, Beijing Institute of Technology) for their useful discussions.

Supporting Information Available: Additional figures and details. This material is available free of charge *via* the Internet at http://pubs.acs.org.

REFERENCES AND NOTES

1. Huang, X.; Qi, X. Y.; Boey, F.; Zhang, H. Graphene-Based Composites. *Chem. Soc. Rev.* **2012**, *41*, 666–686.
2. Huang, X.; Yin, Z. Y.; Wu, S. X.; Qi, X. Y.; He, Q. Y.; Zhang, Q. C.; Yan, Q. Y.; Boey, F.; Zhang, H. Graphene-Based Materials: Synthesis, Characterization, Properties, and Applications. *Small* **2011**, *7*, 1876–1902.
3. Li, B.; Cao, X. H.; Ong, H. G.; Cheah, J. W.; Zhou, X. Z.; Yin, Z. Y.; Li, H.; Wang, J. L.; Boey, F.; Huang, W.; *et al.* All-Carbon Electronic Devices Fabricated by Directly Grown Single-Walled Carbon Nanotubes on Reduced Graphene Oxide Electrodes. *Adv. Mater.* **2010**, *22*, 3058–3061.
4. Chen, C.; Cai, W. M.; Long, M. C.; Zhou, B. X.; Wu, Y. H.; Wu, D. Y.; Feng, Y. J. Synthesis of Visible-Light Responsive Graphene Oxide/TiO_2 Composites with p/n Heterojunction. *ACS Nano* **2010**, *4*, 6425–6432.
5. Mukherji, A.; Seger, B.; Lu, G. Q.; Wang, L. Z. Nitrogen Doped $Sr_2Ta_2O_7$ Coupled with Graphene Sheets as Photocatalysts for Increased Photocatalytic Hydrogen Production. *ACS Nano* **2011**, *5*, 3483–3492.
6. Novoselov, K. S.; Geim, A. K.; Morozov, S. V.; Jiang, D.; Zhang, Y.; Dubonos, S. V.; Grigorieva, I. V.; Firsov, A. A. Electric Field Effect in Atomically Thin Carbon Films. *Science* **2004**, *306*, 666–669.
7. Berger, C.; Song, Z. M.; Li, X. B.; Wu, X. S.; Brown, N.; Naud, C.; Mayou, D.; Li, T. B.; Hass, J.; Marchenkov, A. N.; *et al.* Electronic Confinement and Coherence in Patterned Epitaxial Graphene. *Science* **2006**, *312*, 1191–1196.
8. Reina, A.; Jia, X. T.; Ho, J.; Nezich, D.; Son, H. B.; Bulovic, V.; Dresselhaus, M. S.; Kong, J. Large Area, Few-Layer Graphene Films on Arbitrary Substrates by Chemical Vapor Deposition. *Nano Lett.* **2009**, *9*, 30–35.
9. Cao, X. H.; Shi, Y. M.; Shi, W. H.; Lu, G.; Huang, X.; Yan, Q. Y.; Zhang, Q. C.; Zhang, H. Preparation of Novel 3D Graphene Networks for Supercapacitor Applications. *Small* **2011**, *7*, 3163–3168.

10. Jiao, L. Y.; Zhang, L.; Wang, X. R.; Diankov, G.; Dai, H. J. Narrow Graphene Nanoribbons from Carbon Nanotubes. *Nature* **2009**, *458*, 877–880.
11. Kosynkin, D. V.; Higginbotham, A. L.; Sinitskii, A.; Lomeda, J. R.; Dimiev, A.; Price, B. K.; Tour, J. M. Longitudinal Unzipping of Carbon Nanotubes To Form Graphene Nanoribbons. *Nature* **2009**, *458*, 872–875.
12. Li, X. L.; Zhang, G. Y.; Bai, X. D.; Sun, X. M.; Wang, X. R.; Wang, E.; Dai, H. J. Highly Conducting Graphene Sheets and Langmuir–Blodgett Films. *Nat. Nanotechnol.* **2008**, *3*, 538–542.
13. Liu, N.; Luo, F.; Wu, H. X.; Liu, Y. H.; Zhang, C.; Chen, J. One-Step Ionic-Liquid-Assisted Electrochemical Synthesis of Ionic-Liquid-Functionalized Graphene Sheets Directly from Graphite. *Adv. Funct. Mater.* **2008**, *18*, 1518–1525.
14. Moon, I. K.; Lee, J.; Ruoff, R. S.; Lee, H. Reduced Graphene Oxide by Chemical Graphitization. *Nat. Commun.* **2010**, *1*, 73.
15. Stankovich, S.; Dikin, D. A.; Piner, R. D.; Kohlhaas, K. A.; Kleinhammes, A.; Jia, Y.; Wu, Y.; Nguyen, S. T.; Ruoff, R. S. Synthesis of Graphene-Based Nanosheets *via* Chemical Reduction of Exfoliated Graphite Oxide. *Carbon* **2007**, *45*, 1558–1565.
16. Park, S.; Ruoff, R. S. Chemical Methods for the Production of Graphenes. *Nat. Nanotechnol.* **2009**, *4*, 217–224.
17. Zhou, X. Z.; Huang, X.; Qi, X. Y.; Wu, S. X.; Xue, C.; Boey, F. Y. C.; Yan, Q. Y.; Chen, P.; Zhang, H. *In Situ* Synthesis of Metal Nanoparticles on Single-Layer Graphene Oxide and Reduced Graphene Oxide Surfaces. *J. Phys. Chem. C* **2009**, *113*, 10842–10846.
18. Kim, J.; Cote, L. J.; Kim, F.; Yuan, W.; Shull, K. R.; Huang, J. X. Graphene Oxide Sheets at Interfaces. *J. Am. Chem. Soc.* **2010**, *132*, 8180–8186.
19. Bai, H.; Li, C.; Wang, X. L.; Shi, G. Q. A pH-Sensitive Graphene Oxide Composite Hydrogel. *Chem. Commun.* **2010**, *46*, 2376–2378.
20. Melucci, M.; Treossi, E.; Ortolani, L.; Giambastiani, G.; Morandi, V.; Klar, P.; Casiraghi, C.; Samori, P.; Palermo, V. Facile Covalent Functionalization of Graphene Oxide Using Microwaves: Bottom-Up Development of Functional Graphitic Materials. *J. Mater. Chem.* **2010**, *20*, 9052–9060.
21. Worsley, M. A.; Pauzauskie, P. J.; Olson, T. Y.; Biener, J.; Satcher, J. H.; Baumann, T. F. Synthesis of Graphene Aerogel with High Electrical Conductivity. *J. Am. Chem. Soc.* **2010**, *132*, 14067–14069.
22. Mohanty, N.; Berry, V. Graphene-Based Single-Bacterium Resolution Biodevice and DNA Transistor: Interfacing Graphene Derivatives with Nanoscale and Microscale Biocomponents. *Nano Lett.* **2008**, *8*, 4469–4476.
23. Park, S.; Mohanty, N.; Suk, J. W.; Nagaraja, A.; An, J. H.; Piner, R. D.; Cai, W. W.; Dreyer, D. R.; Berry, V.; Ruoff, R. S. Biocompatible, Robust Free-Standing Paper Composed of a TWEEN/Graphene Composite. *Adv. Mater.* **2010**, *22*, 1736–1740.
24. He, Q. Y.; Sudibya, H. G.; Yin, Z. Y.; Wu, S. X.; Li, H.; Boey, F.; Huang, W.; Chen, P.; Zhang, H. Centimeter-Long and Large-Scale Micropatterns of Reduced Graphene Oxide Films: Fabrication and Sensing Applications. *ACS Nano* **2010**, *4*, 3201–3208.
25. Agarwal, S.; Zhou, X. Z.; Ye, F.; He, Q. Y.; Chen, G. C. K.; Soo, J.; Boey, F.; Zhang, H.; Chen, P. Interfacing Live Cells with Nanocarbon Substrates. *Langmuir* **2010**, *26*, 2244–2247.
26. Chen, W. F.; Yan, L. F.; Bangal, P. R. Chemical Reduction of Graphene Oxide to Graphene by Sulfur-Containing Compounds. *J. Phys. Chem. C* **2010**, *114*, 19885–19890.
27. Pei, S. F.; Zhao, J. P.; Du, J. H.; Ren, W. C.; Cheng, H. M. Direct Reduction of Graphene Oxide Films into Highly Conductive and Flexible Graphene Films by Hydrohalic Acids. *Carbon* **2010**, *48*, 4466–4474.
28. Zhou, T. N.; Chen, F.; Liu, K.; Deng, H.; Zhang, Q.; Feng, J. W.; Fu, Q. A. A Simple and Efficient Method To Prepare Graphene by Reduction of Graphite Oxide with Sodium Hydrosulfite. *Nanotechnology* **2011**, *22*, 45704–45709.
29. Wang, Z. J.; Zhou, X. Z.; Zhang, J.; Boey, F.; Zhang, H. Direct Electrochemical Reduction of Single-Layer Graphene Oxide and Subsequent Functionalization with Glucose Oxidase. *J. Phys. Chem. C* **2009**, *113*, 14071–14075.
30. Akhavan, O.; Ghaderi, E. Photocatalytic Reduction of Graphene Oxide Nanosheets on TiO_2 Thin Film for Photoinactivation of Bacteria in Solar Light Irradiation. *J. Phys. Chem. C* **2009**, *113*, 20214–20220.
31. Dubin, S.; Gilje, S.; Wang, K.; Tung, V. C.; Cha, K.; Hall, A. S.; Farrar, J.; Varshneya, R.; Yang, Y.; Kaner, R. B. A One-Step, Solvothermal Reduction Method for Producing Reduced Graphene Oxide Dispersions in Organic Solvents. *ACS Nano* **2010**, *4*, 3845–3852.
32. Yin, Z. Y.; Wu, S. X.; Zhou, X. Z.; Huang, X.; Zhang, Q. C.; Boey, F.; Zhang, H. Electrochemical Deposition of ZnO Nanorods on Transparent Reduced Graphene Oxide Electrodes for Hybrid Solar Cells. *Small* **2010**, *6*, 307–312.
33. Yin, Z. Y.; Sun, S. Y.; Salim, T.; Wu, S. X.; Huang, X. A.; He, Q. Y.; Lam, Y. M.; Zhang, H. Organic Photovoltaic Devices Using Highly Flexible Reduced Graphene Oxide Films as Transparent Electrodes. *ACS Nano* **2010**, *4*, 5263–5268.
34. Segal, M. Selling Graphene by the Ton. *Nat. Nanotechnol.* **2009**, *4*, 611–613.
35. Wu, J. B.; Agrawal, M.; Becerril, H. A.; Bao, Z. N.; Liu, Z. F.; Chen, Y. S.; Peumans, P. Organic Light-Emitting Diodes on Solution-Processed Graphene Transparent Electrodes. *ACS Nano* **2010**, *4*, 43–48.
36. Xu, Y. X.; Bai, H.; Lu, G. W.; Li, C.; Shi, G. Q. Flexible Graphene Films *via* the Filtration of Water-Soluble Noncovalent Functionalized Graphene Sheets. *J. Am. Chem. Soc.* **2008**, *130*, 5856–5857.
37. Qi, X. Y.; Pu, K. Y.; Zhou, X. Z.; Li, H.; Liu, B.; Boey, F.; Huang, W.; Zhang, H. Conjugated-Polyelectrolyte-Functionalized Reduced Graphene Oxide with Excellent Solubility and Stability in Polar Solvents. *Small* **2010**, *6*, 663–669.
38. Qi, X. Y.; Pu, K. Y.; Li, H.; Zhou, X. Z.; Wu, S. X.; Fan, Q. L.; Liu, B.; Boey, F.; Huang, W.; Zhang, H. Amphiphilic Graphene Composites. *Angew. Chem., Int. Ed.* **2010**, *49*, 9426–9429.
39. Liu, J. Q.; Yin, Z. Y.; Cao, X. H.; Zhao, F.; Lin, A. P.; Xie, L. H.; Fan, Q. L.; Boey, F.; Zhang, H.; Huang, W. Bulk Heterojunction Polymer Memory Devices with Reduced Graphene Oxide as Electrodes. *ACS Nano* **2010**, *4*, 3987–3992.
40. Liu, J. Q.; Lin, Z. Q.; Liu, T. J.; Yin, Z. Y.; Zhou, X. Z.; Chen, S. F.; Xie, L. H.; Boey, F.; Zhang, H.; Huang, W. Multilayer Stacked Low-Temperature-Reduced Graphene Oxide Films: Preparation, Characterization, and Application in Polymer Memory Devices. *Small* **2010**, *6*, 1536–1542.
41. Eda, G.; Chhowalla, M. Chemically Derived Graphene Oxide: Towards Large-Area Thin-Film Electronics and Optoelectronics. *Adv. Mater.* **2010**, *22*, 2392–2415.
42. Shao, Y. Y.; Wang, J.; Engelhard, M.; Wang, C. M.; Lin, Y. H. Facile and Controllable Electrochemical Reduction of Graphene Oxide and Its Applications. *J. Mater. Chem.* **2010**, *20*, 743–748.
43. Kim, F.; Cote, L. J.; Huang, J. X. Graphene Oxide: Surface Activity and Two-Dimensional Assembly. *Adv. Mater.* **2010**, *22*, 1954–1958.
44. Becerril, H. A.; Mao, J.; Liu, Z.; Stoltenberg, R. M.; Bao, Z.; Chen, Y. Evaluation of Solution-Processed Reduced Graphene Oxide Films as Transparent Conductors. *ACS Nano* **2008**, *2*, 463–470.
45. Williams, G.; Seger, B.; Kamat, P. V. TiO_2-Graphene Nanocomposites. UV-Assisted Photocatalytic Reduction of Graphene Oxide. *ACS Nano* **2008**, *2*, 1487–1491.
46. Park, S.; An, J. H.; Jung, I. W.; Piner, R. D.; An, S. J.; Li, X. S.; Velamakanni, A.; Ruoff, R. S. Colloidal Suspensions of Highly Reduced Graphene Oxide in a Wide Variety of Organic Solvents. *Nano Lett.* **2009**, *9*, 1593–1597.
47. Paredes, J. I.; Villar-Rodil, S.; Martinez-Alonso, A.; Tascon, J. M. D. Graphene Oxide Dispersions in Organic Solvents. *Langmuir* **2008**, *24*, 10560–10564.
48. Stankovich, S.; Piner, R. D.; Nguyen, S. T.; Ruoff, R. S. Synthesis and Exfoliation of Isocyanate-Treated Graphene Oxide Nanoplatelets. *Carbon* **2006**, *44*, 3342–3347.
49. Ramm, M.; Ata, M.; Gross, T.; Unger, W. X-ray Photoelectron Spectroscopy and Near-Edge X-ray-Absorption Fine

Structure of C60 Polymer Films. *Appl. Phys. A* **2000**, *70*, 387–390.
50. Ferrari, A. C. Raman Spectroscopy of Graphene and Graphite: Disorder, Electron–Phonon Coupling, Doping and Nonadiabatic Effects. *Solid State Commun.* **2007**, *143*, 47–57.
51. Wang, H. L.; Robinson, J. T.; Li, X. L.; Dai, H. J. Solvothermal Reduction of Chemically Exfoliated Graphene Sheets. *J. Am. Chem. Soc.* **2009**, *131*, 9910–9911.
52. Yang, D. X.; Velamakanni, A.; Bozoklu, G. L.; Park, S. J.; Stoller, M.; Piner, R. D.; Stankovich, S.; Jung, I.; Fieldd, D. A.; Ventrice, C. A., Jr.; *et al.* Chemical Analysis of Graphene Oxide Films after Heat and Chemical Treatments by X-ray Photoelectron and Micro-Raman Spectroscopy. *Carbon* **2009**, *47*, 145–152.
53. Matsumoto, Y.; Koinuma, M.; Ida, S.; Hayami, S.; Taniguchi, T.; Hatakeyama, K.; Tateishi, H.; Watanabe, Y.; Amano, S. Photoreaction of Graphene Oxide Nanosheets in Water. *J. Phys. Chem. C* **2011**, *115*, 19280–19286.
54. Jeong, H. Y.; Kim, J. Y.; Kim, J. W.; Hwang, J. O.; Kim, J. E.; Lee, J. Y.; Yoon, T. H.; Cho, B. J.; Kim, S. O.; Ruoff, R. S.; *et al.* Graphene Oxide Thin Films for Flexible Nonvolatile Memory Applications. *Nano Lett.* **2010**, *10*, 4381–4386.
55. Hummers, W. S.; Offeman, R. E. Preparation of Graphitic Oxide. *J. Am. Chem. Soc.* **1958**, *80*, 133918.
56. Zhou, X.; Huang, X.; Qi, X.; Wu, S.; Xue, C.; Boey, F. Y. C.; Yan, Q.; Chen, P.; Zhang, H. *In Situ* Synthesis of Metal Nanoparticles on Single-Layer Graphene Oxide and Reduced Graphene Oxide Surfaces. *J. Phys. Chem. C* **2009**, *113*, 10842–10846.